Novel Type of Phase Transition in a System of Self-Driven Particles

T. **Vicsek**, A. Czirók, E. Ben-Jacob, I. Cohen, O. Shochet

Physical Review Letters
7. August 1995
4 Pages

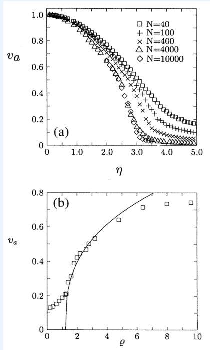

Collective Motion

T. **Vicsek**, A. Zafeiris

Physics Report
6. March 2012
70 Pages

Meta-Analysis

A flocking algorithm for multi-agent systems with connectivity preservation under hybrid metric-topological interactions

Chenlong He, Zuren Feng, Zhigang Ren

Plos One
1. February 2018
23 Pages

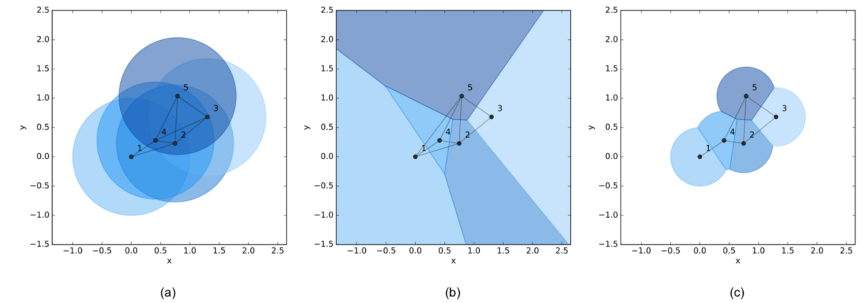

Fig 1. Different types of proximity graphs. The interaction topology of a multi-agent system with 5 agents represented as three types of proximity graphs. (a) *r*-disk graph. (b) Delaunay graph. (c) *r*-limited Delaunay graph.

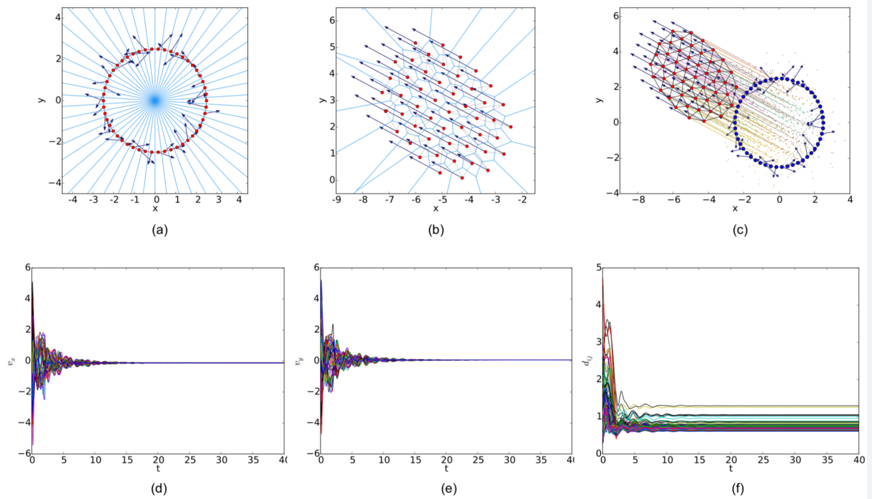

Fig 16. Simulation results of the flocking algorithm based on the Delaunay graph with a circular initial configuration. (a) initial configuration. (b) final configuration. (c) evolution of the multi-agent system. (d) consensus of velocity in *x* component. (e) consensus of velocity in *y* component. (f) variations of relative distances between neighbors.

Phase Transitions in Models of Bird Flocking

H. Christodoulidi, K. van der Weele, Ch.G. Antonopoulos and T. Bountis

Physical Review E
17. September 2018
11 Pages

The aim of the present paper is to elucidate the transition from collective to random behaviorn exhibited by various mathematical models of bird flocking.
In particular, we compare Vicsek's model [Viscek, Phys. Rev. Lett. (1995)] with one based on topological considerations.
The latter model is found to exhibit a first order phase transition from flocking to decoherence, as the "noise parameter" of the problem is increased, whereas Viscek's model gives a second order transition. Refining the topological model in such a way that birds are influenced mostly by the birds in front of them, less by the ones at their sides and not at all by those behind them (because they do not see them), we find a behavior that lies in between the two models.
Finally, we **propose a novel mechanism for preserving the flock's cohesion, without imposing artificial boundary conditions or attracting forces.**

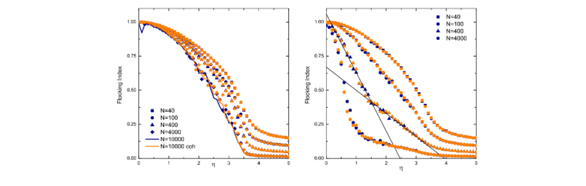

Figure 2: The flocking index as a function of the noise level η for (a) Vicsek's model and (b) the topological model with $n = 7$ interacting neighbors. Both panels show the flocking index for different system sizes N. With blue we represent the random initial conditions and with orange the coherent ones. The two straight lines in the right plot are guides to the eye, illustrating the sudden jump of slope in the curve of the flocking index for $N = 400$.

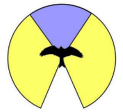

Figure 4: The visual field of a starling is divided in three regions: the binocular (blue), the monocular (yellow) and the visionless area (blank).

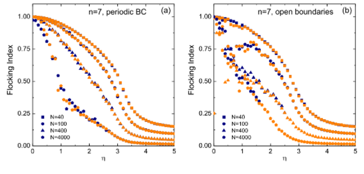

Figure 5: Flocking index for $n = 7$ neighbors versus the noise strength η for different group sizes N of the VRI model with (a) periodic and (b) open boundary conditions. The blue data points represent the random initial conditions and the orange points the coherent ones.

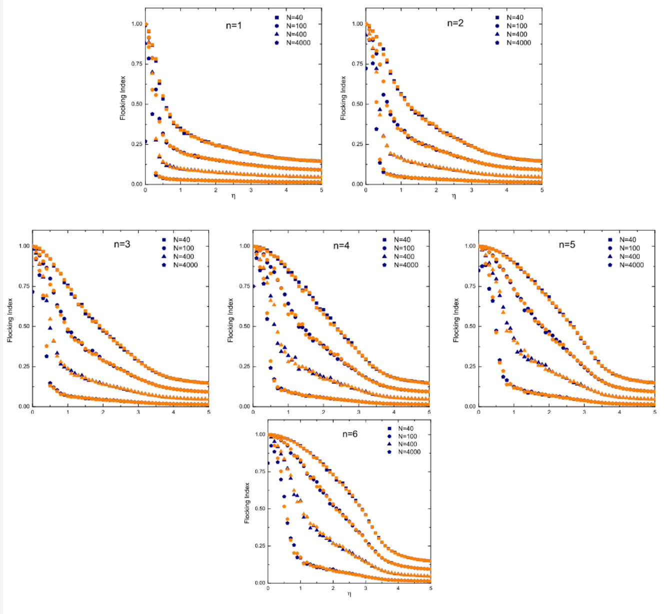

Figure 3: Flocking index versus the noise level η for the topological model (see also Fig. 2(b)) for $n = 1$ to $n = 6$ interacting neighbors respectively. Evidently the curves appear to attain a similar form for $n \geq 3$.

Efficient Flocking: Metric Versus Topological Interactions

V. Kumar and R. De

bioRxiv
24. September 2021
7 Pages

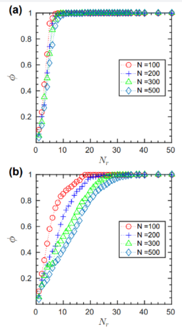

FIG. 4. **Topological interaction**: the order parameter, ϕ, at steady state as a function of number of interacting topological neighbours, N_r, for varying flock sizes, $N = 100, 200, 300, 500$ and initial flock speed, V_0, (a) at a lower speed ($V_0 = 0.01$) and (b) at a higher speed ($V_0 = 1.0$).

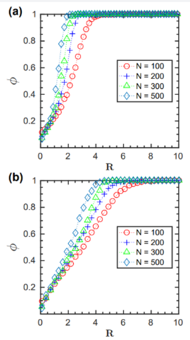

FIG. 3. **Metric interaction**: the order parameter, ϕ, at steady state as a function of interaction radius, R, for different flock size, $N = 100, 200, 300, 500$ and initial speed, V_0, (a) at a lower speed ($V_0 = 0.01$) and (b) at a higher speed ($V_0 = 1.0$).

Phase Transitions in Systems of Self-Propelled Agents and Related Network Models

M. Aldana, V. Dossetti, C. Huepe, V. M. Kenkre, and H. Larralde

Physical Review Letters
2. March 2007
4 Pages

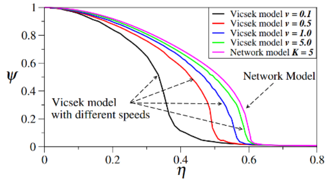

FIG. 1 (color online). Phase diagram of the Vicsek model and the vectorial network model for the case in which the noise is added as in Eq. (1). When the speed v of the particles in the Vicsek model increases, the phase transition converges to that of the vectorial network model. The numerical simulations were carried out for systems with $N = 20\,000$ particles and an average number of interactions per particle $K = 5$.

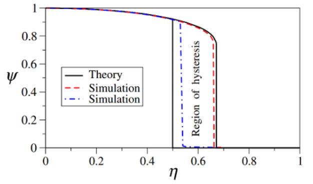

FIG. 3 (color online). Phase diagram of the vectorial network model for the case in which the noise is added as in Eq. (2). The solid line corresponds to the prediction obtained from Eq. (4). The dashed and dotted-dashed curves are the results of the numerical simulation starting out the dynamics from initial conditions for which $\psi(0) \approx 1$ and $\psi(0) \approx 0$, respectively. The phase transition in this case is clearly discontinuous.

Interesting, but most likely not relevant

Emergent synchronization and flocking in purely repulsive self-navigating particles

M. Casiulis and D. Levine

Physical Review E
31. October 2022
17 Pages

Flocking behavior can manifest in a system of particles, even in the exclusive presence of repulsive forces.

Excerpt:
"Inspired by groups of animals and robots, we study the collective dynamics of large numbers of active particles, each one trying to get to its own randomly placed target, while avoiding collisions with each other. [...] For a wide range of parameters, these particles form synchronised system-wide chiral flocks, in spite of the absence of explicit alignment interactions. We show that this dramatic behavior obtains for different system sizes and density, that it is robust against the addition of noise, polydispersity, and bounding walls, and that it can exhibit dynamical topological defects."

Collective Motion and Self-Organization of a Swarm of UAVs: A Cluster-Based Architecture

Z. Ali , Z. Han, and R. Masood

MDPI
31. May 2021
19 Pages

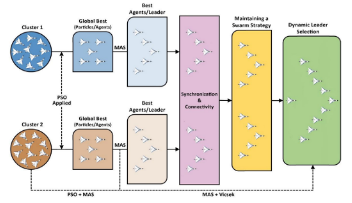

Figure 3. The architecture of the proposed solution.

Learning to Swarm with Knowledge-Based Neural Ordinary Differential Equations

T. Jiahao, L. Pan and M. Hsieh

arXiv
6. September 2021
8 Pages

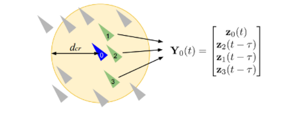

Fig. 1. Decentralized information network for robot 0 with time delay τ, and 3 active neighbors. The image shows robot 0's egocentric view, where 8 neighbors are within its communication range d_{cr}. Only the closest three neighbors contribute to the information structure of robot 0. Their states from $t - \tau$ are ordered based on their proximity to robot 0 to form $\mathbf{Y}_0(t)$.

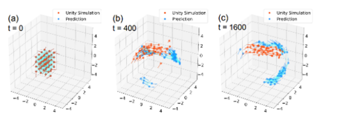

Fig. 9. The flocking of 50 robots using the learnt controller ($d_{cr} = 2, k = 6$) with uniformly initialized positions. The subfigures (a)(b)(c) show the swarm at $t = 0, 400$, and 1600. The light blue lines connect the neighbors.

Evidence of a robust universality class in the critical behavior of self-propelled agents: Metric versus topological interactions

L. Barberis and E. V. Albano

Physical Review E
21. November 2013
6 Pages

Relevance of Metric-Free Interactions in Flocking Phenomena

F. Ginelli and H. Chaté

arXiv
16. September 2010
5 Pages